

# Optical switching in a resonant Fabry–Perot saturable absorber

Yongan Tang<sup>1</sup>, Azad Siahmakoun<sup>1</sup>, Granieri Sergio<sup>1</sup>,  
Mircea Guina<sup>2</sup> and Markus Pessa<sup>2</sup>

<sup>1</sup> Center for Applied Optics Studies, Rose-Hulman Institute of Technology, Terre Haute, IN 47803, USA

<sup>2</sup> Optoelectronics Research Centre, Tampere University of Technology, 33101 Tampere, Finland

E-mail: [Azad.Siahmakoun@rose-hulman.edu](mailto:Azad.Siahmakoun@rose-hulman.edu)

Received 28 April 2006, accepted for publication 18 September 2006

Published 18 October 2006

Online at [stacks.iop.org/JOptA/8/991](http://stacks.iop.org/JOptA/8/991)

## Abstract

We experimentally demonstrate optical switching in a Fabry–Perot saturable absorber using a pump–probe technique. The saturable absorbers are multiple quantum wells, 35 and 42 pairs of alternating layers of 7 nm thick compressively strained Ga<sub>0.42</sub>In<sub>0.58</sub>AsP. These quantum wells are separated by 8 nm thick InP barriers. The reflectivity of these samples as a function of the input optical power is theoretically and experimentally investigated. A switching rate of better than 20 MHz is observed. This optical switching is based on the mechanism of controlling the reflectivity of the Fabry–Perot saturable absorber, while operating at its resonant wavelength, by the pump power. Optical switching speed of 10 ns is possible.

**Keywords:** optical switching, Fabry–Perot cavity, multiple-quantum wells

(Some figures in this article are in colour only in the electronic version)

## 1. Introduction

Vertical Fabry–Perot saturable absorbers (FPSAs) [1] are becoming attractive devices for optical switching and short optical pulse generation [2, 3] due to their ease of fabrication, fast response time, and system implementation. The FPSA is a surface-normal vertical cavity with a multiple quantum well (MQW) saturable absorber. There are two types of FPSA for a range of operating wavelength: anti-resonant FPSA (A-FPSA) and resonant FPSA (R-FPSA), based on the cavity resonance conditions. Although both the A-FPSA and R-FPSA have a broad spectral range, the A-FPSA exhibits minimum optical loss and group delay dispersion, while the R-FPSA exhibits considerable group delay dispersion and maximum nonlinearity.

The MQW saturable absorber in an A-FPSA has a shorter effective interaction length with the optical field than that of an R-FPSA. The A-FPSA also exhibits negligible group delay dispersion (GDD) with less than 20 fs<sup>2</sup> over the entire high-reflectivity bandwidth (800–1100 nm). Consequently, A-FPSAs have been extensively investigated

and developed [3–9] for application in passively mode-locked solid-state lasers [7, 9, 10], while the R-FPSAs or near R-FPSAs [10] introduce considerable GDD in the laser cavity and they are incompatible with solid-state laser technology. However, the longer effective interaction length of the optical field in the R-FPSA leads to greater nonlinearity. The effect of nonlinearity enhancement in R-FPSAs has potential for realizing low threshold optical switching.

The maximum nonlinearity of the R-FPSA is achieved by the combined effect of the asymmetric Fabry–Perot cavity and the MQWs. An asymmetric Fabry–Perot cavity is usually formed by a less reflective front mirror with a reflectivity  $R_f$  and a back semiconductor distributed Bragg reflector (DBR) [11] with an almost 100% reflectivity  $R_b$ . The DBR is formed by piling pairs of quarter-wavelength ( $\lambda/4$ ) layers that are composed of semiconductors with alternating high and low refractive indices ( $n$ ). The reflectivity of the DBR is dependent on the number of piled layers and the difference in the refractive index ( $\Delta n$ ) of the adjacent layers. The front mirror reflectivity  $R_f$  determines the amount of light entering the saturable absorber and therefore controls the

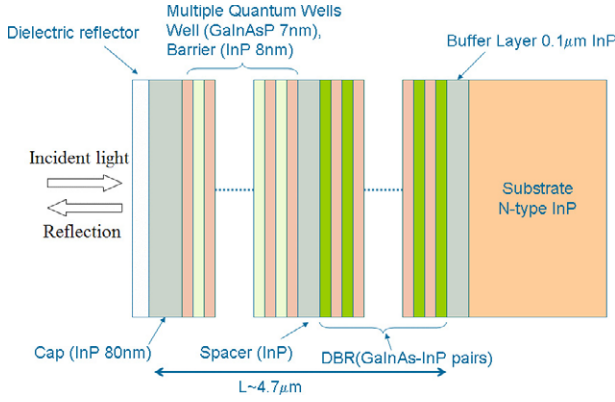


**Figure 1.** A sketch of the MQW-FPSA structure. It consists of a front dielectric reflector, a DBR as the back mirror, and multiple quantum wells in the cavity.

nonlinear reflectivity. The nonlinear and linear absorption are also controlled by the absorbing layers or quantum wells, which have higher nonlinearity and lower saturation energy than bulk absorbers. The finesse of the FPSA is determined by the absorption coefficient of the MQWs,  $R_b$  and  $R_f$ . The absorption recovery time is another important parameter in optical switching and/or optical short pulse generation. There are several methods to reduce the recovery time, such as low-temperature growth, dopant concentration, and ion implantation [12]. For example, the ion implantation method can reduce the recovery time from tens of nanoseconds to the picosecond range.

In this paper, our experimental results show that there is a minimum in the reflectivity curve as a function of input optical power in R-FPSA samples which verifies the theoretical prediction of our model. We also demonstrate the optical switching capability of the R-FPSA samples. This property suggests new opportunities for implementation of R-FPSAs for optical computing, communications, and logic device applications.

## 2. FPSA structure and properties

The FPSA structure (shown in figure 1) was grown by solid-source molecular beam epitaxy on an S-doped n-type InP(100) substrate at the Optoelectronic Center of Tampere University in Finland. The back mirror is a DBR consisting of 19.5 pairs of quarter-wavelength layers of  $n^+$ -Ga<sub>0.47</sub>In<sub>0.53</sub>As and InP, which have a refractive index difference ( $\Delta n$ ) of  $\sim 0.42$ . This DBR has a broad stopband of wavelength range from 1.525 to 1.610  $\mu\text{m}$  with 96% reflectivity. The saturable absorber is an MQW which has alternating layers of 7 nm thick compressively strained Ga<sub>0.42</sub>In<sub>0.58</sub>AsP quantum wells separated by an 8 nm InP barrier. The MQWs have a saturation fluence of about 250  $\mu\text{J cm}^{-2}$ , and short recovery time of  $\sim 10$  ns. The optical length of the Fabry–Perot cavity is controlled by placing an InP spacer layer and a cap layer (InP) which are under and atop of the MQWs, respectively. The front mirror is a dielectric reflector with reflectivity about 70%. The cavity length is about 4.7  $\mu\text{m}$ , and its free spectral range (FSR) is about 260 nm. The maximum finesse of these samples that depends on the absorption of the MQWs is about 16.

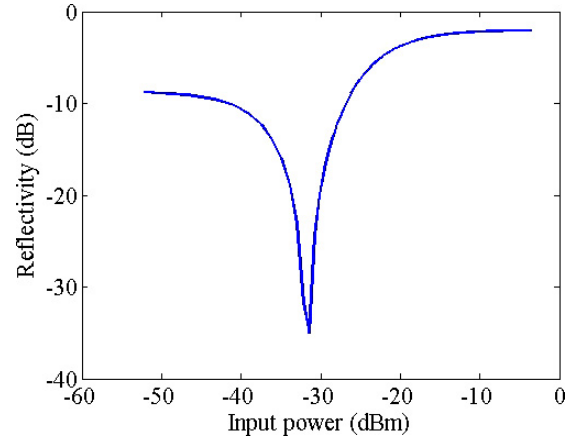


**Figure 2.** The reflectivity of the FPSA as a function of input power. Notice the minimum reflectivity occurs near  $-30$  dBm ( $1 \mu\text{W}$ ).

## 3. Theoretical model

For such a cavity, and using the plane-wave approximation at normal incidence, the reflectivity  $R$  is given by the following equation [13]:

$$R = \frac{B + F \sin^2 \phi}{1 + F \sin^2 \phi} \quad (1)$$

where

$$B = \frac{R_f \left[ 1 - \left( \frac{R_\alpha}{R_f} \right) \right]^2}{(1 - R_\alpha)^2} \quad (2)$$

$$F = \frac{4R_\alpha}{(1 - R_\alpha)^2} \quad (3)$$

$$R_\alpha = \sqrt{R_f R_b} e^{-\alpha d} \quad (4)$$

$$\alpha = \frac{\alpha_0}{1 + P/P_{\text{sat}}} \quad (5)$$

where  $\phi$  is the phase detuning of the light travelling in the FPSA,  $R_f$  is the reflectivity of the front mirror,  $R_b$  is the reflectivity of the back mirror,  $\alpha$  is the absorption coefficient,  $d$  is the thickness of the saturable absorber,  $\alpha_0$  is the small signal absorption coefficient,  $P$  is the input optical power, and  $P_{\text{sat}}$  is the saturation optical power.

The R-FPSA has maximum nonlinearity when the reflectivity  $R$  is at its minimum value [14]. In the case of an R-FPSA, this requires that the phase detuning is zero,  $\phi = 0$ , for the resonant wavelength. Therefore equation (1) becomes

$$R = \frac{R_f \left[ 1 - \left( \frac{R_\alpha}{R_f} \right) \right]^2}{(1 - R_\alpha)^2}. \quad (6)$$

Equation (6) predicts that the cavity reflectivity approaches zero when  $R_\alpha = R_f$ . This condition can be achieved by changing the input optical power. This is due to the fact that the absorption coefficient  $\alpha$  depends on the input optical power (see equation (5)). By inserting the condition  $R_\alpha = R_f$  into equation (4), one can obtain

$$R_f = R_b e^{-2\alpha d} = R_b e^{-\frac{2\alpha_0 d}{1 + P/P_{\text{sat}}}}. \quad (7)$$

Equation (7) describes that there exists a specific value of optical power for which the absorption  $\alpha$  satisfies the minimal reflectivity. From equation (6), a plot of the FPSA reflectivity for different input optical power is shown in figure 2. The simulation parameters are  $\alpha_0 = 0.95 \text{ m}^{-1}$ ,  $d = 0.39 \mu\text{m}$ ,

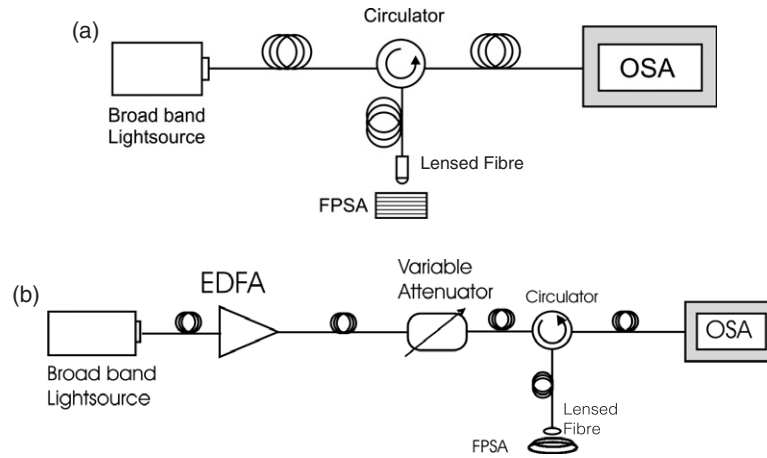


**Figure 3.** Experimental setup for (a) the spectral distribution of the low-intensity reflectivity and (b) the reflectivity measurements of the FPSA samples. EDFA: erbium-doped fibre amplifier, OSA: optical spectrum analyser.

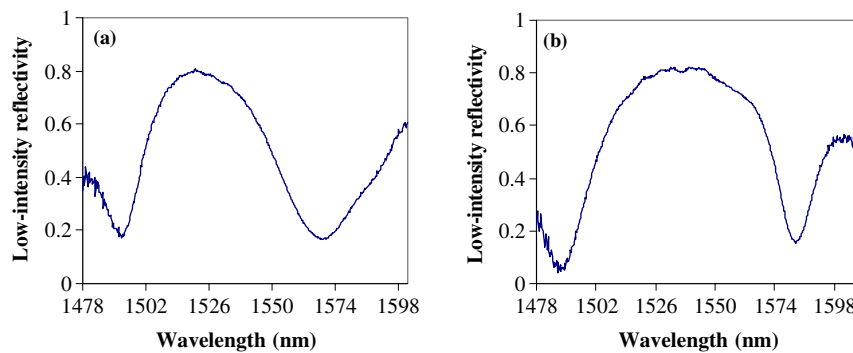


**Figure 4.** Low-intensity reflectivity spectrum of two R-FPSA samples in the C-band, (a) sample with 35 QWs with one resonance wavelength at 1573 nm, (b) sample with 42 QWs with one resonance wavelength at 1583 nm.

$R_b = 0.96$ ,  $R_f = 0.7$ , and  $P_{\text{sat}} = 0.5 \mu\text{W}$ . These parameters are chosen to have values close to the actual parameters of the R-FPSA sample. The notch in this figure reveals that the device can be tuned to an OFF-state due to the absorption by the MQWs at a certain value of input power.

#### 4. Experiments

The low-intensity reflectivity measurements of the FPSA are made by using a broadband light source (1400–1700 nm) and the setup shown in figure 3(a). The light from the broadband source enters a three-port optical circulator and then is focused on the FPSA sample by a lensed-fibre. The reflected light from the FPSA is collected by the same fibre lens and sent to an optical spectrum analyser via the output port of the optical circulator. The spectral distribution of the low-intensity reflection of sample (a) with 35 quantum wells (QWs) and sample (b) with 42 QWs are shown in figures 4(a) and (b) respectively. The stopband of the DBR is between 1525 nm and 1610 nm for both samples. While the resonant wavelengths are estimated to be  $1573.5 \pm 0.5$  nm and  $1583.7 \pm 0.3$  nm as seen in figure 4.

In order to study the change in the reflectivity of these FPSA samples at different optical power density, the setup

is modified, as shown in figure 3(b). The light from the broadband source is now amplified by an erbium-doped fibre amplifier (EDFA); IPG Model EAD-500CL. The amplified light enters a variable optical attenuator which is utilized to control the input optical power into the R-FPSA. By changing the variable optical attenuator, a set of reflection values of the broadband spectrum is acquired for different input optical power directed onto the FPSA. The reflectivity measurements of the FPSA, sample a with 35 QWs, including losses in the measurement system are shown in figure 5(a). These curves show the spectral distribution of the reflectivity within the range of 1547–1603 nm and for five different power levels:  $-12$ ,  $-15$ ,  $-32$ ,  $-48$ ,  $-57$  dBm. Figure 5(b) shows the sample reflectivity for two near-resonance wavelengths, 1572.83 and 1574.44 nm, as a function of optical input power. These experimental results show that this R-FPSA has a minimum reflectivity of about  $-11.5$  dB at an input power of  $-32$  dBm. Notice that below or above this input power level, the reflectivity increases, revealing a minimum, as predicted by equation (6). These measurements show a minimum in the reflectivity curve, whose shape is in good agreement with the theoretical simulation given in figure 2. However, the depth of the notch in the experimental measurement is shallower than that of the simulation. This could be due to background noise, and/or coupling losses from FPSA to the fibre lens.

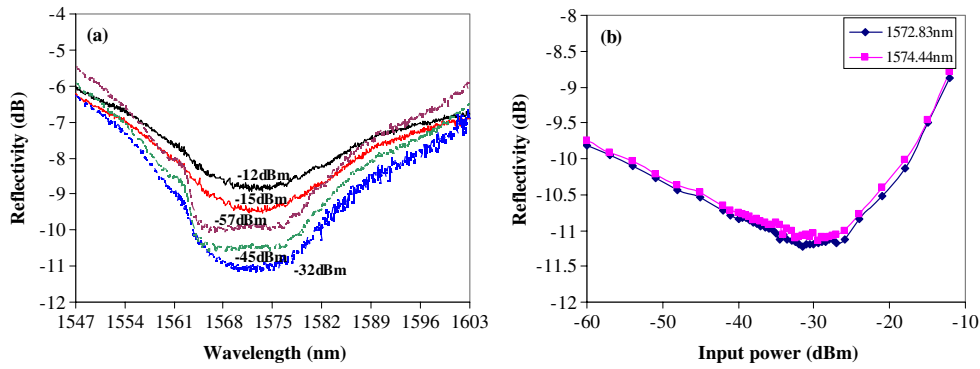


**Figure 5.** (a) The reflectivity of the R-FPSA as a function of the input optical power for sample a. (b) The reflectivity of the R-FPSA versus different input power at two wavelengths near the resonance of sample a.

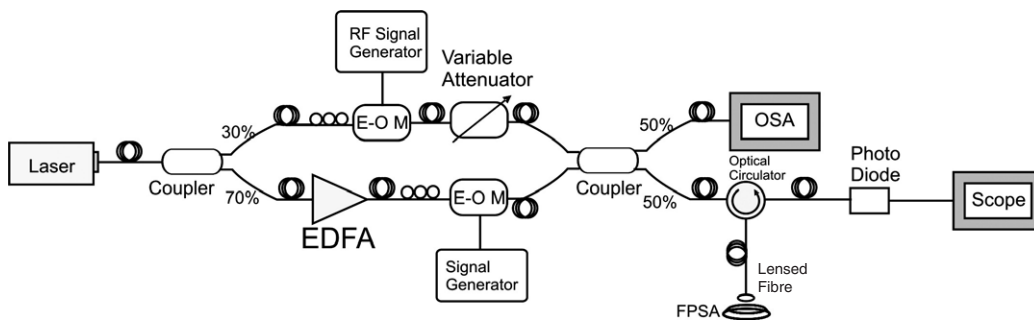


**Figure 6.** The optical switching experimental setup; EOM is electro-optical modulator.

An optical switching experiment is designed based on the above observation of the minimum reflectivity in the R-FPSA. The experimental setup is shown in figure 6. A Santec model MLS-2000 tunable laser is operated at output power of 5 dBm at the resonant wavelength, 1573.7 nm, of the FPSA. The light is split into two by a  $2 \times 2$  70/30 fibre-optic coupler. The lower power from the coupler, the signal (probe) beam, is modulated sinusoidally by an electro-optics modulator (EOM) at 30 MHz. The power level of this signal beam is controlled by a variable optical attenuator. The second output (70%) from the  $2 \times 2$  coupler, the pump beam, is amplified by the EDFA and then modulated by a second EOM that is driven by a square wave at 5 MHz. A 50/50  $2 \times 2$  coupler is utilized to combine the signal beam and the pump beam. One output port from this coupler is directed onto the FPSA through an optical circulator and the lensed-fibre. Then the reflection from the FPSA is sent to an oscilloscope through the optical circulator and a photodiode. The OSA is utilized for monitoring the input optical power and its spectrum.

The experimental result of the optical switching using the setup shown in figure 6 is presented by figure 7. In this experiment, the optical power of the sinusoidally modulated signal is  $-32$  dBm ( $0.6 \mu\text{W}$ ) while the pump beam acting as a clock at 5 MHz has an average optical power of  $-2$  dBm ( $0.63$  mW). Notice that the average power of the signal beam corresponds to the minimum reflectivity observed in the reflectivity of the FPSA and is shown in figure 5(a). It is also shown in figure 5(a) that the FPSA reflectivity for a 10 nm range of wavelength (1567–1577 nm) is similar to that of the near-resonant wavelength at 1573.7 nm. Therefore optical

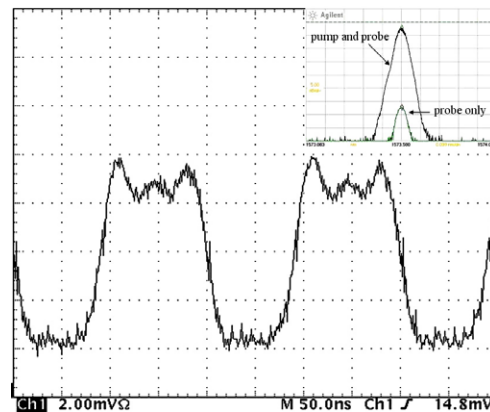


**Figure 7.** A sinusoidal probe beam is switched ON/OFF by the square-wave pump. Inset: optical spectrum of the input probe signal with and without pump. The signal is about 1 mV peak-to-peak in a scale of 2.00 mV/division. The baseline represents zero volts, providing a contrast ratio of better than 0.7.

switching can be achieved with this R-FPSA for an input wavelength of  $1573 \pm 5$  nm. However, the maximum switching bandwidth is limited by our instrumentations and for the most part by the EOM. Ignoring the rise-time of the optoelectronic instruments, the switching bandwidth of these FPSAs is limited by their recovery time ( $\sim 10$  ns for our samples) and is about 100 MHz. The modulated sinusoidal signal is switched ON when the pump beam is turned on, and it is OFF when the pump beam is turned off, as can be seen in figure 7.

## 5. Conclusions

The reflectivity of an R-FPSA is theoretically investigated and the simulation shows that there is a minimum in the reflectivity versus the input optical power. This property is verified experimentally by using a broadband light source. The ON and OFF states of the FPSA device are demonstrated by a pump–probe technique. An optical switching experiment is arranged with a modulated signal beam of optical power  $-32$  dBm at 30 MHz. A switching time of  $\sim 50$  ns is easily obtained with an average pump power of  $-2$  dBm. One advantage of this optical switching system is its ability to switch ON/OFF for a very weak signal ( $-32$  dBm). The lower limit of switching speed could not be verified due to equipment limitations at this time. However, the physical limitation in the switching speed is due to the 10 ns recovery time of the MQWs which can be reduced by adding dopants. Meanwhile, we intend to demonstrate the feasibility of the FPSA as a high-speed optical switch for potential applications such as optical computing, communications and logic devices.

## References

- [1] Keller U, Weingarten K J, Kartner F X, Kopf D, Braun B, Jung I D, Fluck R, Honninger C, Matuschek N and Au J A 1996 Semiconductor saturable absorber mirrors (SESAM's) for femtosecond to nanosecond pulse generation in solid-state lasers *IEEE J. Sel. Top. Quantum Electron.* **2** 435–53
- [2] Xiang N, Guina M D, Vainionpää A M, Lyytikäinen J, Suomalainen S, Saarinen M J, Okhotnikov O, Sajavaara T and Keinonen J 2002 Broadband semiconductor saturable absorber mirrors in the  $1.55\text{-}\mu\text{m}$  wavelength range for pulse generation in fiber lasers *IEEE J. Quantum Electron.* **38** 369–74
- [3] Jung I D, Fartner F X, Matuschek N, Sutter D H, Morier-Genoud F, Shi Z, Scheuer V, Tilsch M, Tschudi T and Keller U 1997 Semiconductor saturable absorber mirrors supporting sub-10-fs pulses *Appl. Phys. B* **65** 137–50
- [4] Jung I D, Kärtner F, Brovelli L, Kamp M, Keller U and Moser M 1995 Scaling of the antiresonant Fabry–Perot saturable absorber design toward a thin saturable absorber *Opt. Lett.* **20** 1859–61
- [5] Haiml M, Grange R and Keller U 2004 Optical characterization of semiconductor saturable absorbers *Appl. Phys. B* **79** 331–9
- [6] Schön S, Haiml M, Gallmann L and Keller U 2002 Fluoride semiconductor saturable-absorber mirror for ultrashort pulse generation *Opt. Lett.* **27** 1845–7
- [7] Aschwanden A, Lorenser D, Unold H, Paschotta R, Gini E and Keller U 2005 2.1-W picosecond passively mode-locked external-cavity semiconductor laser *Opt. Lett.* **30** 272–4
- [8] Grange R, Rutz A, Liverini V, Hamil M, Schön S and Keller U 2005 Nonlinear absorption edge properties of  $1.3\text{-}\mu\text{m}$  GaInNAs saturable absorbers *Appl. Phys. Lett.* **87** 132103
- [9] Rutz A, Grange R, Liverini V, Hamil M, Schön S and Keller U 2005  $1.5\text{-}\mu\text{m}$  GaInNAs semiconductor saturable absorber for passively modelocked solid-state lasers *Electron. Lett.* **41** 321–3
- [10] Okhotnikov O and Guina M 2000 Stable single- and dual-wavelength fiber laser modelocked and spectrum shaped by a Fabry–Perot saturable absorber *Opt. Lett.* **25** 1624–6
- [11] Brovelli L R and Keller U 1995 Simple analytical expressions for the reflectivity and the penetration depth of a Bragg mirror between arbitrary media *Opt. Commun.* **116** 343–50
- [12] Delpon E L, Oudar J L, Bouche N, Raj R, Shen A, Stelmakh N and Lourtioz J M 1998 Ultrafast excitonic saturable absorption in ion-implanted InGaAs/InAlAs multiple quantum wells *Appl. Phys. Lett.* **72** 759–61
- [13] Whitehead M, Parry G and Wheatly P 1989 Investigation of etalon effects in GaAs–AlGaAs multiple quantum well modulators *IEE Proc. Pt. J.* **136** 52–8
- [14] Whitehead M and Parry G 1989 High-contrast reflection modulation at normal incidence in asymmetric multiple quantum well Fabry–Perot structure *Electron. Lett.* **25** 566–8